Charging of atoms, clusters, and molecules on metal-supported oxides: A general and long-ranged phenomenon

Pentti Frondelius,[1] Anders Hellman,[2] Karoliina Honkala,[1,3] Hannu Häkkinen,[1,3] and Henrik Grönbeck[2,*]
[1]*Department of Physics, Nanoscience Center, P.O. Box 35, University of Jyväskylä, FIN-40014 Jyväskylä, Finland*
[2]*Competence Centre for Catalysis and Department of Applied Physics, Chalmers University of Technology, SE-41296 Göteborg, Sweden*
[3]*Department of Chemistry, Nanoscience Center, P.O. Box 35, University of Jyväskylä, FIN-40014 Jyväskylä, Finland*
(Received 28 May 2008; published 20 August 2008)

The density-functional theory is used to investigate the adsorption of Au atoms, Au clusters, and NO_2 molecules on transition-metal-supported oxides. As compared to unsupported oxides, the adsorbates on supported oxide films are charged and experience a higher adsorption energy. The origin of the effect is explored by considering two different oxides (MgO and Al_2O_3) and a range of supporting metals. Moreover, the limits of the enhancement are probed by explicit calculations for thick MgO films and low coverage. The long-range character of the phenomenon is attributed to electrostatic polarization. The absolute strength depends on several contributions and their relative importance changes with system composition.

DOI: 10.1103/PhysRevB.78.085426 PACS number(s): 73.22.−f, 71.15.Mb, 73.30.+y

I. INTRODUCTION

Over the past few years it has become clear that thin metal-oxide layers supported on metal substrates exhibit chemical characteristics in pronounced variance with the corresponding bulk oxide surfaces. On the basis of density-functional-theory (DFT) calculations, it was predicted that gold atoms on MgO(100) supported on Mo should be charged and adsorbed with a higher adsorption energy than on bulklike (unsupported) MgO(100).[1,2] The prediction of charging has been confirmed experimentally by scanning tunneling microscopy (STM) measurements.[3,4] The effect has been theoretically shown to apply for Au clusters of various sizes[5–8] on MgO/Mo as well as on MgO/Ag.[9] The general nature of the phenomenon was demonstrated by its presence for molecules with high enough electronic affinity (e.g., NO_2) adsorbed on different oxides [MgO,[10] BaO,[11] and Al_2O_3 (Ref. 12)] supported on Ag or Pt.

The implications of charging and stabilization could potentially be of importance for the understanding and design of heterogeneous catalysts. In applications, catalysts are often realized as metal particles dispersed on an oxide and model systems are designed with the oxide supported on metals. By varying the thickness of a metal-supported oxide, the charge state of the metal phase could be modified.[13] Moreover, in high surface area oxides (such as γ-Al_2O_3), the effect could be active between neighboring pores. In this way it could change the properties of molecular adsorption.

Although numerous reports have appeared on the stabilization effect, a clear picture on its origin and the importance of different contributions is missing. In the original work it was proposed that the mechanism is a consequence of direct tunneling of one electron from the metal through the oxide to the adsorbate.[1] Instrumental in this scenario is the reduction in the metal work function when coated by an oxide film.[14,15] However, a recent report on NO_2 adsorption on Al_2O_3/Ag demonstrated that the effect is active despite an increased work function when Al_2O_3 is grown on Ag.[12] It has also been stressed that the charging introduces marked structural relaxations at the oxide/metal interface and that the electron originates from this region.[10–12] This part of the effect depends on the interaction between the oxide and the metal and, thus, the choice of oxide and metal. Moreover, it has been pointed out that the charging of the adsorbate strongly polarizes the oxide.[16] Without the presence of screening mechanisms (e.g., polarizable electron charge in a color center), the polarization can lead to long-range interaction between the charged adsorbate and the supporting metal.[16]

In a simplistic picture, the adsorption energy (E_{ads}) of an atom, a cluster, or a molecule (A) on a metal oxide (MO) supported by a metal (M) can be decomposed according to

$$E_{ads} \sim E_{pol} + E_b[A/\mathrm{MO}] + E_{adh}[\mathrm{MO}/M] + (\mathrm{EA} - \Phi) + E[A/A]. \quad (1)$$

Here, E_{pol} is the electrostatic contribution owing to the polarization of the oxide and the image charge in the metal. In addition to the electrostatic contribution, there is a direct chemical interaction between the adsorbate and the oxide (E_b). This interaction may change depending on the charge state of the adsorbate. Another contribution is the oxide/metal interface energy ($E_{adh}[\mathrm{MO}/M]$), which may be modified when an electron is abstracted from the MO/M system. The stabilization should also depend on the difference between the electronic affinity (EA) of the adsorbate and the work function (Φ) of the combined MO/M system. It is clear that charged adsorbates on the oxide will interact repulsively, $E[A/A]$, and that the stabilization energy should depend on the adsorbate coverage. Note that the adsorbate charging is a crucial component in all terms in Eq. (1).

The first term in Eq. (1) is electrostatic polarization. The polarization energy E_{pol} between a point charge (q) placed z_1 above an interface is given by (atomic units)[17]

$$E_{pol} = \frac{q^2}{4\varepsilon_1 z_1}\frac{\varepsilon_1 - \varepsilon_2}{\varepsilon_1 + \varepsilon_2}. \quad (2)$$

ε_1 and ε_2 are the dielectric constants of the surrounding medium and the (bulk) surface, respectively. If ε_2 is larger than ε_1, the charge is stabilized by the interface. In the limit of a metal (large ε_2), this expression reduces to the energy gain

TABLE I. Used lattice constants (a) for the considered metals and lattice mismatches (γ) between the metal (100) surface and MgO(100).

	Mo	Ag	Pd	Au	Pt
a (Å) (PBE)	3.17	4.13	3.96	4.15	4.00
a (Å) (RPBE)	3.19	4.14	3.99	4.18	4.00
γ (%) (PBE)	4.3	−4.0	−7.9	−3.5	−7.0
γ (%) (RPBE)	4.7	−3.7	−7.2	−3.5	−7.0

experienced by a charged particle outside a conducting plane.

In the context of metal oxidation, Stoneham and Tasker[18] (ST) examined a continuum model for the effect of a second boundary, i.e., a charged particle outside an oxide in contact with a metal. It was found that a metal support could stabilize substantially the charged particle. For a point charge placed 2 Å above the oxide surface, the extra energy owing to a metal support is 1.55 eV. Because the ST model includes a dependence on distance similar to Eq. (2), the stabilization is long ranged.

Although the continuum model captures the qualitative effect of the oxide polarization and the image charge created in the metal, the other terms in Eq. (1) are not included. In order to investigate the different aspects of these contributions, we have applied first-principles calculations for a number of model systems. In particular, we explore the effects of: (i) oxide thickness, (ii) adsorbate coverage, (iii) choice of oxide, (iv) choice of metal, and (v) electron affinity of the adsorbate.

II. COMPUTATIONAL METHOD AND SYSTEMS

The calculations are performed within the pseudopotential plane-wave implementation of the DFT. In particular, the DACAPO code is used.[19] The exchange-correlation functional is approximated with the Perdew-Burke-Ernzerhof (PBE) expression[20] for NO_2 adsorption, whereas the revised Perdew-Burke-Ernzerhof (RPBE) form[21] is applied for Au adsorption. Ultrasoft pseudopotentials are used to describe the interaction between the valence electrons and the atomic cores.[22] The Kohn-Sham orbitals are expanded in plane waves up to a kinetic energy of 25 Ry.

MgO in the bulk phase has a rocksalt structure. The lattice constant (within both PBE and RPBE) is calculated to be equal to 4.30 Å. This is slightly larger than the experimental value of 4.21 Å, but it is in good agreement with previously reported DFT results.[23] For α-Al_2O_3, a hexagonal unit cell[24] is applied. It consists of six hexagonal-closed-packed O layers. Al ions are placed in 2/3 of the octahedral vacancies between the O layers. The optimized lattice constants (PBE) for the hexagonal unit cell are $a=4.80$ and $c=13.11$ Å, which agree with other DFT results.[25] The corresponding experimental values are $a=4.76$ and $c=13.00$ Å.[24] The used lattice constants for the considered metals are reported in Table I. Note that the crystal structure of Mo is bcc, whereas the other metals are fcc.

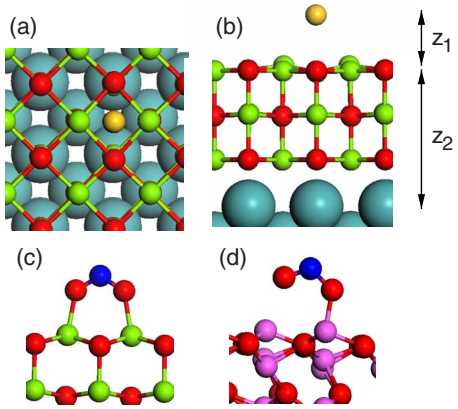

FIG. 1. (Color online) Structural models of investigated systems. (a) and (b) are top and side views of Au adsorbed on 3MgO/Mo. (c) and (d) are structural models for NO_2 adsorbed on MgO and Al_2O_3, respectively. z_1 is the distance between adsorbate and the oxide top layer and z_2 is the distance between the supporting metal and the top layer of the oxide. Atomic color codes: Au (orange), Mo (blue green), Al (pink), Mg (green), N (blue), and O (red).

Single-crystal and metal-supported MgO(100) films are modeled at different thicknesses using three surface cells, namely, $p(2\times2)$, $p(3\times3)$, and $p(5\times5)$. Adsorption on the unsupported $Al_2O_3(0001)$ film is studied with a $p(2\times2)$ surface cell. Reciprocal-space integration over the Brillouin zone is approximated with finite sampling using the Monkhorst-Pack scheme.[26,27] The number of applied k points depends on the size of the surface cell and the metallic nature of the system. For $p(2\times2)$ surface cells, a $(4\times4\times1)$ sampling is employed. For larger surface cells, a $(2\times2\times1)$ sampling is applied for supported MgO(100), whereas the Γ-point approximation is applied for unsupported oxide films. For $Al_2O_3(0001)$, a $(4\times4\times1)$ sampling is used in all cases.

The unsupported oxide films are studied with surface cells built from the corresponding oxide lattice constant. For the supported films, the size of the surface cell is determined by the lattice constant of the metal. MgO is supported with the oxygen anions located directly over the metal atoms; see Fig. 1. Several studies have confirmed that this configuration is the stable structure.[28,29] The mismatch between the metal and MgO(100) surfaces is moderate in all cases; see Table I. For the $Al_2O_3(0001)$ film, a $\sqrt{3}\times\sqrt{3}R30°$ metal (111) slab is used. Ag is positioned below Al atoms and the lattice mismatch between Ag(111) and the oxide is ~5%.

Whereas the adsorbates in the gas phase are treated spin polarized, the adsorption is calculated without spin polarization. Explicit calculations for Au on three oxides layers on Mo(100) [3MgO/Mo] at a coverage of 0.11 ML shows that the effect of spin polarization on the adsorption energy is within 0.05 eV. NO_2 adsorption energy has a similar dependence upon spin polarization. Repeated slabs are separated by more than 12 Å. To describe the situation of a surface terminated from bulk, the bottom layer of the slab is fixed to the bulk-truncated structure. All the other atoms in the cell are allowed to relax during the geometry optimizations. The optimized systems have residual forces below 0.05 eV/Å.

The adsorption energy (E_{ads}) of an adsorbate A is calculated according to

$$E_{ads} = E[A] + E[\text{slab}] - E[A/\text{slab}]. \quad (3)$$

Here, $E[A/\text{slab}]$ is the total energy of the combined system, $E[A]$ is the energy of A in gas phase, and $E[\text{slab}]$ is the energy of the slab without adsorbate. Thus, a positive value corresponds to exothermic adsorption. Charge transfer is analyzed with the Bader method,[30,31] which separates the total electron density onto the atoms in the system. The reliability of this method for similar systems has been demonstrated earlier.[6,7]

III. ADSORPTION ON UNSUPPORTED OXIDES

The most stable adsorption site for an Au atom on MgO(100) is atop an oxygen anion (O-top). It was early recognized that the adsorption energy of metal atoms on MgO(100) converges fast with oxide thickness.[32] Here, the Au adsorption energy is calculated to be 0.56 eV for a three-layer MgO(100) film at a coverage of 0.11 ML. This is in agreement with the RPBE result in Ref. 33.

At 0.25 ML coverage, the adsorption energy of NO_2 on a five-layer MgO(100) [Al_2O_3(0001)] slab is calculated to be 0.36 eV (0.54 eV). The coverage on Al_2O_3(0001) is related to the number of Al ions. The ground-state structures on the two oxides differ (see Fig. 1): In the case of MgO(100), NO_2 binds in a bridge fashion, where the two O atoms coordinate toward adjacent Mg cations. Owing to the larger spatial separation between Al cations on alumina, only one O atom is coordinated to an Al cation on Al_2O_3(0001). The O-N-O angle is 127° and 121° for MgO and Al_2O_3, respectively. The difference in angle is consistent with a difference in charge transfer from the oxide to NO_2. The Bader analysis reveals a charge transfer of 0.3 (0.6) electrons for MgO (Al_2O_3). As the lowest unoccupied molecular orbital (LUMO) level of NO_2 has an O-O bonding character, the O-N-O angle is a sensitive measure of charging. In gas phase, the angle is 134° for the neutral molecule and 115° for the nitrite (NO_2^-).

IV. ADSORPTION ON METAL-SUPPORTED OXIDES

The aim of the present study is to explore the roles of different contributions to the adsorption energy of Au clusters and NO_2 on thin oxide layers supported on metal surfaces. In the following, the effects of (i) oxide thickness, (ii) adsorbate coverage, (iii) choice of oxide, (iv) choice of metal, and (v) electron affinity of the adsorbate are investigated. The results are put in context by comparisons with the ST continuum model.[18]

A. Effect of oxide thickness

Previous studies of an Au atom adsorption on metal-supported MgO films[1,2,16] have established that (a) the metal support induces charging of Au, (b) the metal support enhances E_{ads}, and (c) the stable adsorption site is a hollow site on the supported thin oxide films, whereas it is O-top on the bulk oxide. The charging and the change in adsorption site have been observed experimentally.[3,4] Here, the convergence of Au adsorption properties on MgO/Mo(100) with increasing film thickness are investigated by explicit calculations. In particular, films of up to 20 layers (~40 Å) are considered for a coverage of 0.25 ML.

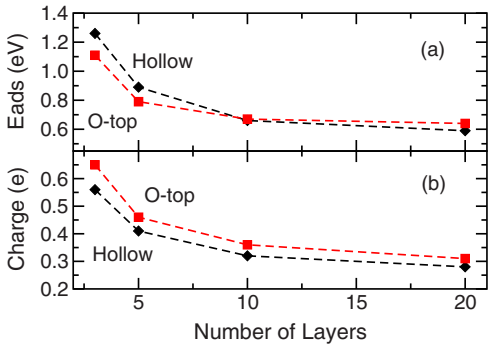

FIG. 2. (Color online) Au atom adsorption energy (a) and charge (b) as a function of MgO layers supported on Mo(100). The adsorbate coverage is 0.25 ML.

Figure 2 shows the Au adsorption energy and charge for hollow and O-top sites. For a three-layer film, the hollow site is preferred, with an adsorption energy of 1.26 eV. On the 20-layer film, the most stable site is O-top and the adsorption energy is 0.64 eV. The preferred adsorption site changes at the ten-layer thick film of MgO. This agrees with experimental observations for Au adsorption on MgO/Ag(100), where the change in adsorption site takes place between three and eight MgO layers.[3] The difference in the adsorption energy between 10 and 20 layers is only 0.03 eV (0.07 eV) for the O-top (hollow) site. Hence, E_{ads} is already close to converged for 10 layers. There is still a slight difference between the results for 20 layers and a single-crystal MgO surface. At the same coverage, the adsorption energy on a bulk MgO(100) surface is 0.46 eV. With a lattice constant corresponding that of Mo(100), E_{ads} is 0.55 eV. The difference between hollow and O-top is 0.12 eV on the single-crystal MgO surface and 0.05 eV on 20 ML MgO/Mo. The slight difference between the thick supported and single-crystal MgO(100) surfaces suggests that the numerical accuracy in these large calculations is within 0.1 eV.

The Au charging decreases as a function of oxide thickness. The projected density of states supports this observation: The Au 6*s* state moves toward the Fermi level with increasing number of MgO layers and is singly occupied for the 20-layer case. On 20MgO/Mo, the excess charge on Au is 0.28 electrons, which is close to the value calculated for unsupported MgO(100) and is in agreement with the experimental estimates of neutrality.[34]

B. Effect of adsorbate coverage

Because of the charging, the electrostatic adsorbate-adsorbate interaction is repulsive. For Au atoms on MgO/Ag it has been demonstrated experimentally that the interaction results in an ordered superstructure.[3] Here, the effect of adsorbate-adsorbate interactions is investigated by calculating Au adsorption on 3MgO/Mo at different coverages rang-

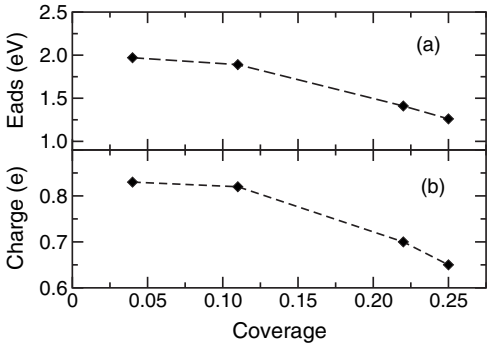

FIG. 3. Au atom adsorption energy (a) and charge (b) as a function of adsorbate coverage for Au on 3MgO/Mo(100).

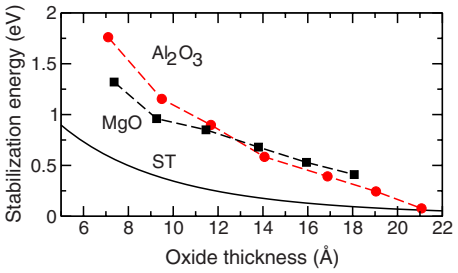

FIG. 4. (Color online) Stabilization energy for NO_2 adsorbed on Ag(100)-supported MgO (squares) and Al_2O_3 (circles) as a function of oxide thickness (z_2 in Fig. 1). The solid line is the stabilization predicted by the ST model.

ing from 0.04 to 0.25 ML. The former value is close to the experimental coverage reported in Ref. 3.

Figure 3 displays how E_{ads} and Au charging depend on coverage for adsorption at the hollow site. A decrease in the coverage from 0.25 to 0.04 ML results in a strengthening of the adsorption by 0.71 eV. A lower coverage is accompanied by a higher amount ($\sim 0.2e$) of charging. It should be noted that the difference in adsorption properties for 0.04 and 0.11 ML coverages is small: E_{ads} decreases by 0.08 eV and the excess charge by $0.01e$. This justifies *post priori* the use of a 0.11 ML coverage for studies of isolated Au atoms often assumed in the literature.[1,2,6,7,16]

In Ref. 3, the radial pair distribution function of adsorbates was measured to have the first peak at 16 Å. Moreover, the probability of observing Au atoms at distances smaller than 10 Å was found to be negligible.[3] The present results support this observation. In a homogeneously distributed system, the 0.04 ML case corresponds to an adsorbate-adsorbate nearest-neighbor distance of ~16 Å and a sign of adsorbate repulsion is present for 0.11 ML. The results in Fig. 3 demonstrate the competition between Au repulsion and Au bonding to MgO/Mo. Although the adsorption energy is enhanced by increased charge transfer, the repulsive interaction is substantial and prevents complete charging at high enough coverage.

C. Choice of oxide

So far, we have discussed the stabilization of adsorbates on a metal-supported MgO oxide. Previously, the mechanism has shown to be valid also for Pt-supported BaO.[11] However, the alkali-earth metal oxides are structurally simple, and it is important to investigate whether the mechanism is active also for other types of oxides.

As one part of the stabilization can be attributed to effects incorporated in the ST continuum model, it is interesting to note that the only oxide property that enters in the model is the dielectric constant. Most oxides have a dielectric constant close to 10. In this respect, the stabilization effect should not depend strongly on the type of oxide. To verify this, an additional oxide with different properties as compared to those of the alkali-earth oxides was considered, namely, Al_2O_3. The stabilization energies for NO_2 on Ag-supported MgO and Al_2O_3 are shown in Fig. 4. The stabilization is calculated as the difference in E_{ads} between the supported film and bulk oxide surfaces. With the exception of the thinnest films, the bond enhancement is similar for both oxides. The stabilization effect of NO_2 adsorbed on metal-supported oxides resembles that of the Au atom; so does the charging pattern.

In Fig. 4, the first-principles results are compared with the results from the ST model.[18] Here, the dielectric constants for the oxide and the metal are taken to be 10 and 100, respectively. Because the ST model requires the adsorbate charge for each oxide thickness, we interpolate the calculated charging values for 2MgO/Ag ($0.9e$) and unsupported MgO ($0.3e$) with an exponential fit. Even if the ST results indicate a long-range interaction, the absolute stabilization is severely underestimated. This indicates that the bond enhancement is a phenomenon where all the terms in Eq. (1) are of importance.

D. Choice of supporting metal

A decisive component in the stabilization mechanism is the charging of an adsorbate. Thus, the work function of the combined oxide/metal system should be an important parameter. To investigate this, we calculate the adsorption of Au and NO_2 on two layers of MgO supported by Mo, Pd, Pt, Ag and Au.

Figure 5(a) shows the calculated work functions of the clean (100) metal surfaces and the case where MgO is deposited on the metal. The work function of the metals ranges from 4.1 eV (Mo) to 5.6 eV (Pt). Because MgO induces polarization at the interface, it lowers the work function by ~2 eV. The variation in E_{ads} for Au and NO_2 as a function of work function is presented in Fig. 5(b). Although the calculated values are scattered, there is a tendency that a low work function is associated with a high adsorption energy. The Bader analysis [Fig. 6(a)] reveals that the amount of charge transferred to Au or NO_2 is almost independent of the supporting metal and work function (~0.9 electrons). The effect of supporting metal is instead shown in E_{ads} because the energy penalty for electron abstraction depends on system composition. The charge on the adsorbate originates both from the oxide and the metal. Figure 6(b) shows a decomposition of the charge depletion. Roughly, 2/3 of the charge is abstracted from the metal.

It should be noted that no reduction in work function is calculated for metal-supported Al_2O_3. On the contrary, the

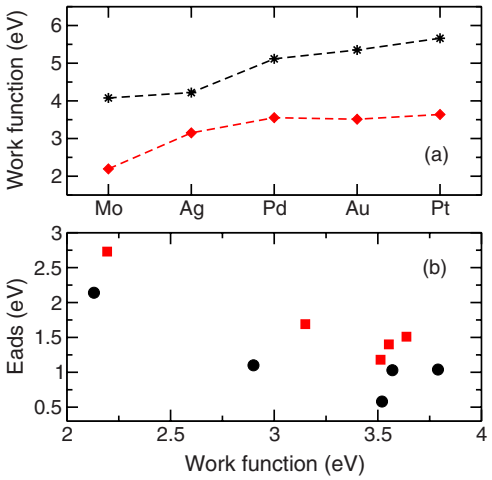

FIG. 5. (Color online) (a) Calculated (PBE approximation) work functions for Mo, Ag, Pd, Au, and Pt (stars) and the corresponding metal-supported 2MgO systems (diamonds). (b) Adsorption energy for Au (circles) and NO_2 (squares) as a function of work function. The results for Au adsorption are obtained within RPBE, whereas NO_2 adsorption is treated within the PBE approximation.

work function is increased. The work function for two layers of Al_2O_3 on Ag(111) is calculated to be 5.0 eV and only a moderate variation (0.3 eV) is calculated as a function of oxide film thickness. Thus, the different nature of the bonding at Al_2O_3/Ag as compared to that at MgO/Ag results in an increased work function: At the Al_2O_3/Ag interface, Ag is located at the cation and charge is polarized toward the oxide. For the MgO/Ag interface, Ag is positioned below oxide anions, which induce a compression of the electron density.

E. Effect of electron affinity

As adsorbate charging is the crucial component of the mechanism, it is reasonable that the effect should depend on the electron affinity (EA) of the adsorbates. Indeed for MgO/Mo it was shown that, whereas an Au atom (EA =2.3 eV) is negatively charged, a Pd atom (EA=0.56 eV) is close to neutral.[1] This result was confirmed experimentally.[3]

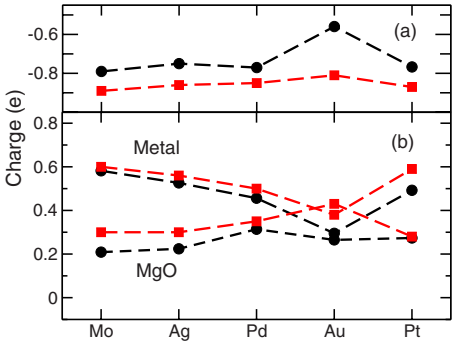

FIG. 6. (Color online) (a) The amount of charge transferred to Au (circles) and NO_2 (squares) for adsorption onto two layers of MgO on different supporting metals. (b) Decomposition of the abstracted charge into MgO and supporting metal.

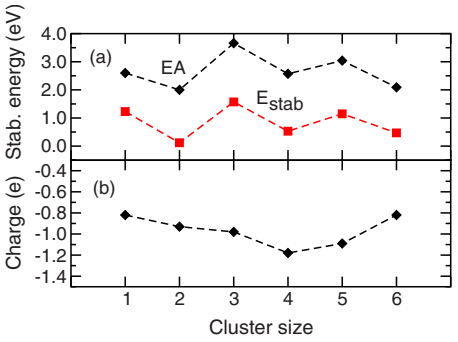

FIG. 7. (Color online) Stabilization energy owing to the metal as a function of Au cluster size (a) and the corresponding charging (b) for adsorption on three layers of MgO supported by Mo(100). The stabilization energy is compared with the electronic affinity (EA) of the gas-phase clusters.

It was recently shown that the adsorption energy of the Au clusters up to the hexamer on MgO/Mo correlates closely with the EA of the clusters.[6,7] The EA oscillates as a function of cluster size and so does the adsorption energy; see the upper panel of Fig. 7. However, the amount of charge transferred to a cluster does not correlate with EA; instead it is close to one electron for all cluster sizes.

V. DISCUSSION

In Sec. I, the adsorption energy was decomposed into five terms: the polarization of oxide and metal, direct binding between the oxide and the adsorbate, the modification of oxide-metal adhesion, difference between EA and Φ, and direct adsorbate-adsorbate interaction. Sections II–IV exemplified the different contributions and it is clear that the calculated stabilization energy depends on all the terms. It is difficult to rank the importance of the contributions: All the terms depend on the adsorbate charging and are linked to each other. For example, charging of the adsorbate is associated with the polarization of the oxide and the polarization is accompanied with structural changes. None of the phenomena occurs without the others. Furthermore, the significance of the different contributions may be system dependent. Despite this complexity, some general conclusions can be made.

The important contributions are the polarization of the oxide and the formation of an image charge in the metal.[1,15] These contributions are qualitatively captured by the ST continuum model. In the original ST model, the charge is unity. If the charge is parameterized with the Bader charges calculated for Au adsorption on MgO/Mo(100) at 0.25 coverage, stabilization energies of 0.45, 0.18, 0.09, and 0.05 eV are obtained for 3, 5, 10, and 20 layers, respectively. These should be compared to the first-principles results of 0.71, 0.33, 0.11, and 0.04 eV. Thus, the long-range character of the stabilization can be attributed to polarization of the oxide and metal. Note, however, that the good agreement for the thicker film must be regarded as fortuitous: In addition to assuming zero coverage, the ST model does not include the energy penalty associated with the abstraction of an electron from the MO/M system, (EA$-\Phi$) in Eq. (1).

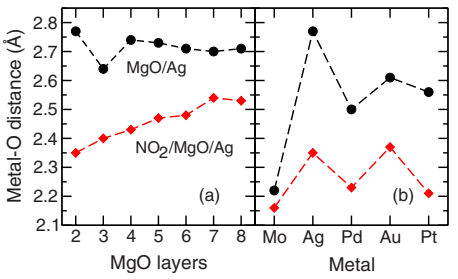

FIG. 8. (Color online) Metal-O distance between the supporting metal and MgO at the interface as a function of MgO layers supported on Ag(100) (a) and as a function of the metal support with two layers of MgO (b). Results with and without NO_2 are shown as diamonds and circles, respectively.

The systematic investigation of coverage (Fig. 3) shows the energetic balance between the attractive Au/MgO/Mo interaction and the repulsive Au-Au interaction. The charging is reduced with increased coverage owing to adsorbate-adsorbate interactions.

The oxides considered here have an ionic character and adsorbate charging modifies the direct adsorbate-oxide bond. A structural signature of this is the pronounced oxide relaxation around the adsorbate on a metal-supported oxide. In fact, the energetic contribution from the structural relaxation is large: The Au adsorption energy on 3MgO/Ag (3MgO/Mo) is 1.11 eV (1.89 eV) and reduces to 0.43 eV (0.94 eV) if the oxide and the metal are not allowed to relax upon Au adsorption. This is in agreement with the results in Ref. 35. A constrained substrate leads to weaker polarization and reduced charge transfer to the adsorbate. Thus, the energy contributions from the structural relaxation and charge transfer are difficult to separate. Some of the energy penalty in the constrained calculations should, however, be attributed to the relaxation at the oxide-metal interface. The size of this relaxation depends on supporting metal, oxide thickness, and adsorbate: NO_2 gives rise to more pronounced relaxations than does Au. In Fig. 8(a) the Ag-O distance at the interface before and after adsorption of NO_2 on MgO/Ag are reported. The Ag-O distance is reduced by 0.2–0.3 Å upon NO_2 adsorption, with the largest reduction calculated for 2MgO/Ag. Figure 8(b) shows the variation in the metal-O distance for different supporting metals. The reduced metal-O distance is a structural signature of an enhanced bonding.[10,11] In fact, analysis of charge difference patterns for NO_2 adsorption on 2MgO/Ag(100) have revealed charge accumulation between the anion in the oxide and Ag.[10] If only the adsorbate and the top oxide layer are allowed to relax, the adsorption energy of NO_2 on 2MgO/Ag is calculated to be 0.89 eV (at 0.25 coverage), which should be compared with 1.66 eV for the fully relaxed system. The corresponding values for NO_2 adsorption on $2Al_2O_3/Ag$ are 0.81 and 2.29 eV, respectively. A similar trend is valid for Au adsorption. If relaxation is allowed only for Au and the topmost MgO layer on 3MgO/Ag (3MgO/Mo), the adsorption energy is 0.59 eV (1.34 eV). A comparison of these results with the values for the completely relaxed and fully constrained substrate suggests that a substantial contribution of the adsorption energy originates from the structural relaxation (and modified bonding) at the oxide/metal interface. The charging of the adsorbate is a prerequisite for a high adsorption energy, which is nicely exemplified by the constrained calculations. Au is charged by $0.81e$ in the fully relaxed 3MgO/Ag system. The value reduces to $0.44e$ when only the topmost layer is relaxed, and for the constrained 3MgO/Ag system the charging is $0.31e$.

Because charge is transferred from the oxide/metal to the adsorbate, $(EA-\Phi)$ is one contribution to the adsorption energy. The dependence on Φ is, however, not straightforward. In Fig. 6 we show that the adsorbate charging does not depend on the supporting metal, i.e., the work function. Moreover, the possible oxide induced decrease in the substrate work function is not a necessity for the stabilization: NO_2 is charged on Al_2O_3/Ag despite the fact that Φ is higher for $Al_2O_3/Ag(111)$ than for Ag(111).[12] Nevertheless, for a given oxide, the stabilization energy correlates to some extent with Φ; see Fig. 5. The dependence on EA in Eq. (1) is much clearer, which is exemplified by the results in Fig. 7.

VI. CONCLUSIONS

To conclude, the density-functional theory has been used to investigate the adsorption of Au atoms, Au clusters, and NO_2 on oxides supported on transition metals. Compared to the unsupported oxides, the adsorbates are charged and experience a higher adsorption energy. The origin of this effect is found to be the consorted action of several contributions where the relative importance of the different parts changes with the system composition. Furthermore, the contributions are linked to each other, which leads to an almost indistinguishable interplay between the different energy terms. However, the long-range character of the effect is attributed to electrostatic polarization.

ACKNOWLEDGMENTS

We thank Michael Walter for useful discussions. We gratefully acknowledge the support from the Academy of Finland, the Swedish Research Council, and the COST D41 network. We thank CSC (Espoo), NSC (Jyväskylä), C3SE (Göteborg), and PDC (Stockholm) for providing CPU time. The Competence Centre for Catalysis is hosted by Chalmers University of Technology and financially supported by the Swedish Energy Agency and the member companies AB Volvo, Volvo Car Corporation, Scania CV AB, GM Powertrain Sweden AB, Haldor Topsoe A/S, and the Swedish Space Corporation.

*Corresponding author; ghj@chalmers.se

[1] G. Pacchioni, L. Giordano, and M. Baistrocchi, Phys. Rev. Lett. **94**, 226104 (2005).
[2] L. Giordano, M. Baistrocchi, and G. Pacchioni, Phys. Rev. B **72**, 115403 (2005).
[3] M. Sterrer, T. Risse, U. M. Pozzoni, L. Giordano, M. Heyde, H.-P. Rust, G. Pacchioni, and H.-J. Freund, Phys. Rev. Lett. **98**, 096107 (2007).
[4] M. Sterrer, T. Risse, M. Heyde, H.-P. Rust, and H.-J. Freund, Phys. Rev. Lett. **98**, 206103 (2007).
[5] D. Ricci, A. Bongiorno, G. Pacchioni, and U. Landman, Phys. Rev. Lett. **97**, 036106 (2006).
[6] P. Frondelius, H. Häkkinen, and K. Honkala, Phys. Rev. B **76**, 073406 (2007).
[7] P. Frondelius, H. Häkkinen, and K. Honkala, New J. Phys. **9**, 339 (2007).
[8] B. Yoon and U. Landman, Phys. Rev. Lett. **100**, 056102 (2008).
[9] L. Giordano and G. Pacchioni, Phys. Chem. Chem. Phys. **8**, 3335 (2006).
[10] H. Grönbeck, J. Phys. Chem. B **110**, 11977 (2006).
[11] P. Broqvist and H. Grönbeck, Surf. Sci. **600**, L214 (2006).
[12] A. Hellman and H. Grönbeck, Phys. Rev. Lett. **100**, 116801 (2008).
[13] H.-J. Freund, Surf. Sci. **601**, 1438 (2007).
[14] J. Goniakowski and C. Noguera, Interface Sci. **12**, 93 (2004).
[15] L. Giordano, F. Cinquini, and G. Pacchioni, Phys. Rev. B **73**, 045414 (2006).
[16] K. Honkala and H. Häkkinen, J. Phys. Chem. C **111**, 4319 (2007).
[17] W. R. Smyth, *Static and Dynamic Electricity* (McGraw-Hill, New York, 1939).
[18] A. M. Stoneham and P. W. Tasker, Philos. Mag. B **55**, 237 (1987).
[19] B. Hammer, L. B. Hansen, and J. K. Nørskov, Phys. Rev. B **59**, 7413 (1999); S. R. Bahn and K. W. Jacobsen, Comput. Sci. Eng. **4**, 56 (2002).
[20] J. P. Perdew, K. Burke, and M. Ernzerhof, Phys. Rev. Lett. **77**, 3865 (1996).
[21] B. Hammer, L. B. Hansen, and J. K. Nørskov, Phys. Rev. B **59**, 7413 (1999).
[22] D. Vanderbilt, Phys. Rev. B **41**, 7892 (1990).
[23] P. Broqvist, H. Grönbeck, and I. Panas, Surf. Sci. **554**, 262 (2004).
[24] R. W. G. Wyckoff, *Crystal Structures* (Wiley, New York, 1963), Vol. 2.
[25] C. Ruberto, Y. Yourdshahyan, and B. I. Lundqvist, Phys. Rev. B **67**, 195412 (2003).
[26] H. J. Monkhorst and J. D. Pack, Phys. Rev. B **13**, 5188 (1976).
[27] J. D. Pack and H. J. Monkhorst, Phys. Rev. B **16**, 1748 (1977).
[28] J. Goniakowski, Phys. Rev. B **59**, 11047 (1999).
[29] H. Grönbeck and P. Broqvist, J. Phys. Chem. B **107**, 12239 (2003).
[30] R. Bader, *Atoms in Molecules: A Quantum Theory* (Oxford University Press, New York, 1990).
[31] G. Henkelman, A. Arnaldsson, and H. Jónsson, Comput. Mater. Sci. **36**, 354 (2006).
[32] V. Musolino, A. Selloni, and R. Car, J. Chem. Phys. **108**, 5044 (1998).
[33] L. M. Molina and B. Hammer, Phys. Rev. B **69**, 155424 (2004).
[34] M. Yulikov, M. Sterrer, M. Heyde, H. P. Rust, T. Risse, H.-J. Freund, G. Pacchioni, and A. Scagnelli, Phys. Rev. Lett. **96**, 146804 (2006).
[35] L. Giordano, U. Martinez, S. Sicolo, and G. Pacchioni, J. Chem. Phys. **127**, 144713 (2007).